Turbulent force as a diffusive field with vortical sources

Jie-Zhi Wu[a)]
The University of Tennessee Space Institute, Tullahoma, Tennessee 37388

Ye Zhou
Institute for Computer Applications in Science and Engineering, NASA Langley Research Center, Hampton, Virginia 23681 and IBM Research Division, T. J. Watson Research Center, P.O. Box 218, Yorktown Heights, New York 10598

Xi-Yun Lu[b)] and Meng Fan[c)]
The University of Tennessee Space Institute, Tullahoma, Tennessee 37388

(Received 9 January 1997; accepted 18 November 1998)

In Reynolds-average Navier–Stokes equation it is the divergence of Reynolds stress tensor, i.e., the turbulent force, rather than the tensor itself, is to be simulated and partially modeled. Thus, directly working on turbulent force could bring significant simplification. In this paper a novel exact equation for incompressible turbulent force **f** is derived: $(\partial/\partial t - \nu\nabla^2)\mathbf{f}=\nabla\cdot\mathbf{S}$, where ν is the molecular viscosity and all source terms in tensor **S** to be modeled are vortical. The dominant mechanism is the advection and stretching (with an opposite sign) of a ''pseudo-Lamb vector'' by fluctuating velocity field. No coupling with pressure is involved. The equation follows from a study of the mean fluctuating Lamb vector and kinetic energy, which constitute the turbulent force. Both constituents are governed by the same kind of equations as **f**. This innovative turbulent-force equation is similar to Lighthill's acoustic analogy and naturally calls one's attention to studying the vortical sources of turbulent force. The methodology described here may lead to turbulence models which provide more complete treatment than that of two-equation models, but relatively easier computation than that of second-order closures. © *1999 American Institute of Physics.* [S1070-6631(99)01303-3]

I. INTRODUCTION

The Reynolds averaged Navier–Stokes (RANS) equation has been the major means in simulating complicated turbulent flows of engineering interest. Large-eddy simulation (LES), though promising in the future, can only deal with relatively simple configurations and low Reynolds numbers within the current computer capacity. Even though they used a highly optimistic estimate, Spalart *et al.*[1] have recently shown that for an airplane wing an LES needs a number of grid points of order of 10^{11} and that of time steps of 5×10^6, which would be feasible only 40 years later according to the present growth rate of computer power. For RANS, algebraic, one-equation or two-equation models have been mainly based on the scalar kinetic energy-dissipation relation. In the transport of kinetic energy and dissipation, the molecular viscosity is replaced by eddy viscosity; but in practice these models have turned out to be inadequate to simulate highly unsteady separated vortical flows. Evidence (e.g., Wu *et al.*[2]) has indicated that some key large-scale vortical structures could be smeared out by a too-large eddy viscosity, so that sometimes the prediction could even be qualitatively questionable.

The highest level of RANS is the second-order closure based on full transport equation of the Reynolds stress.[3] This, however, is still impractical in engineering computations. Moreover, the second-order closure involves several complicated tensor correlations, and an oversimplified modeling of any single term could hamper the entire accuracy of the simulation. Therefore, searching for new approaches to RANS modeling with adequate complexity and robust predictive ability is still an urgent task.

As one of the efforts toward this goal, in this paper we develop an innovative formulation very different from conventional ones. The primary motivation of our approach was the following general mathematic observation. Any vector field **f** in three-dimensional space can be expressed as the divergence of a ''tensor potential,'' say **T**, such that $\mathbf{f}=\nabla\cdot\mathbf{T}$. A given **f** has infinitely many such potentials, which may have up to nine independent components and of which the differences are divergence-free tensors. Among these tensor potentials the simplest one has only three independent components, which are a linear combination of the scalar and vector potentials in the Stokes–Helmhotz (SH) decomposition of **f**. Namely, if

$$\mathbf{f}=\nabla\phi+\nabla\times\boldsymbol{\psi},\quad \nabla\cdot\boldsymbol{\psi}=0,$$

then the simplest tensor potential of **f** is $\hat{T}_{ij}=\delta_{ij}\phi-\epsilon_{ijk}\psi_k$. Thus, if one is interested in **f** only, there is no need for studying its tensor potentials of more than three independent components.

a)Electronic mail: jzwu@utsi.edu
b)Permanent address: Department of Modern Mechanics, University of Science and Technology of China, Hefei, Anhui 230026, China.
c)On leave from State Key Laboratory on Turbulence Research, Peking University, Beijing 100871, China.

The implication of this observation to incompressible turbulence is evident. Let $\mathbf{U}$, $\mathbf{\Omega}$, and $H_0=P+|\mathbf{U}|^2/2$ be the mean velocity, vorticity and stagnation enthalpy, respectively. In the RANS equation with unit density

$$\frac{\partial \mathbf{U}}{\partial t}+\mathbf{\Omega}\times\mathbf{U}=-\nabla H_0-\mathbf{f}+\nu\nabla^2\mathbf{U}, \tag{1a}$$

what really matters is only the turbulent force

$$\mathbf{f}=\nabla\cdot(\overline{\mathbf{u}'\mathbf{u}'}), \tag{1b}$$

rather than the six-component Reynolds stress $\overline{\mathbf{u}'\mathbf{u}'}$ itself. Here and below an overline means ensemble average. Thus, it would be preferable to directly study the former or its SH potentials instead of the latter. This idea was first proposed in an unpublished paper of Wu *et al.*[4] In an unpublished report,[5] Perot and Moin proposed some modeled transport equations for the SH potentials of the turbulent force $\mathbf{f}$ based on the data of direct numerical simulation. They showed that this approach has a computational cost comparable to two-equation models but a predictive ability approaching that of second-order closure.

The study for the SH potentials of turbulent force can be put on a rational basis only if these potentials can be identified as well-defined physical quantities, since then their own transport equations can be derived. For turbulent force this identification is straightforward[6]

$$\mathbf{f}=\overline{\mathbf{u}'\cdot\nabla\mathbf{u}'}=\overline{\mathbf{l}'}+\nabla K, \tag{2}$$

where

$$\overline{\mathbf{l}'}=\overline{\boldsymbol{\omega}'\times\mathbf{u}'}, \tag{3a}$$

$$K=\tfrac{1}{2}\overline{|\mathbf{u}'|^2}, \tag{3b}$$

are the mean fluctuating Lamb vector and kinetic energy, respectively. To split Eq. (2) into the two parts of the SH decomposition, we define an intrinsic transverse-longitudinal decomposition (an SH decomposition) for a vector, denoted by $\mathbf{F}=\mathbf{F}_\perp+\mathbf{F}_\parallel$, such that

$$\nabla\cdot\mathbf{F}_\perp=0, \tag{4a}$$

$$\nabla\times\mathbf{F}_\parallel=0. \tag{4b}$$

As is well known, this splitting is in general not unique; it is invariant under a gauge transformation

$$\mathbf{F}_\perp\rightarrow\tilde{\mathbf{F}}_\perp=\mathbf{F}_\perp+\nabla\psi,\quad \mathbf{F}_\parallel\rightarrow\tilde{\mathbf{F}}_\parallel=\mathbf{F}_\parallel-\nabla\psi,\quad \nabla^2\psi=0.$$

This nonuniqueness does not exist for unbounded flow with uniform condition at infinity or flow with periodic boundary conditions, as can be easily seen in Fourier space. For bounded flow, the arbitrariness comes from the fact that one only has physical boundary conditions for an unsplit vector but not for each split part. Note that it is this freedom that enables introducing a proper artificial boundary condition for ψ, and hence $\mathbf{F}_\perp$ and $\mathbf{F}_\parallel$, which can ensure the exclusion of the gradient of any potential, including pressure, from $\mathbf{F}_\perp$. This interesting issue deserves a separate analysis; thus, in this paper we simply ignore the role of $\nabla\psi$ for neatness.

Now, denoting

$$\overline{\mathbf{l}'}_\parallel=\nabla\chi, \tag{5}$$

the transverse and longitudinal parts of $\mathbf{f}$ are

$$\mathbf{f}_\perp=\overline{\mathbf{l}'}_\perp, \tag{6a}$$

$$\mathbf{f}_\parallel=\nabla(K+\chi). \tag{6b}$$

In contrast to the conventional $K-\epsilon$ models that attempt to represent the whole effect of $\mathbf{f}$, we now see that K only reflects a portion of the longitudinal component of $\mathbf{f}$. The main part of $\mathbf{f}$ is the *vectorial and vortical* $\overline{\mathbf{l}'}$ as it should be, because turbulence is inherently a vectorial and vortical field. While models based on second-order tensors seem to be more than necessary, models based on a scalar equation are inevitably oversimplified.

This being the case, in this paper we focus on the exact transport equation for turbulent force. We proceed as follows, each step containing some new results.

First, in Sec. II we derive the exact transport equations for the full Lamb vector $\mathbf{l}=\boldsymbol{\omega}\times\mathbf{u}$ as well as its mean fluctuating part $\overline{\mathbf{l}'}$. We find that as in the momentum equation, the nonlinear evolution of $\mathbf{l}$ is solely governed by the advection and stretching–tilting (with an opposite sign) of its transverse part. We confirm this observation by a numerical example. Of particular interest is the finding that the equation for $\overline{\mathbf{l}'}$ is extremely simple: A linear diffusion equation with molecular diffusivity and vortical sources, which are decoupled from any longitudinal quantities.

In Sec. III we revisit the transport equation of fluctuating kinetic energy and cast it to the same form as that for $\overline{\mathbf{l}'}$. Then the equation for turbulent force, our kernel result, immediately follows from Eq. (2). It has exactly the same structure as the $\overline{\mathbf{l}'}$-equation, and hence significantly differs from conventional formulations.

We believe that these results set a basis toward a novel direction in turbulence study and modeling. Although the analysis is made for RANS, with minor modification the same idea is well applicable to subgrid-scale modeling in LES.

II. TRANSPORT EQUATIONS FOR LAMB VECTOR AND ITS FLUCTUATIONS

The importance of Lamb vector $\mathbf{l}$ in general fluid dynamics is well known (e.g., Refs. 7 and 8). It is also known that $\mathbf{l}_\parallel$ and $\mathbf{l}_\perp$ play very different roles. In particular, the relevance of Lamb vector and its two parts to turbulent flows has attracted many researchers. For example, the investigations of the Lamb vector was recently focused on its role in topological fluid mechanics.[9,10] Moffatt[11–13] argued that turbulent flow may spend a large portion of its time in a neighborhood of fixed points of steady Euler equations, e.g., solutions of $\nabla h_0=-\mathbf{l}=-\mathbf{l}_\parallel$, where h_0 is the stagnation enthalpy. This proposal was based on an important article by Arnold[14] on magnetohydrodynamics. Using the well-known analogy between the magnetohydrodynamics and the Euler equations for incompressible steady flows of an inviscid fluid, Arnold's result has immediate bearing to the question of existence and structure of solution of the latter. The structure of these unstable Euler flows, in turn, may have some bearing on the problem of the spatial structure of turbulence. Moreover, Several authors have noticed that for fully developed turbulence $\overline{\mathbf{l}'_{\parallel}}$ can be larger than $\overline{\mathbf{l}'}_{\perp}$ (e.g., Refs. 15 and 16 and references therein), especially in the regions with strong enstrophy or dissipation. Then the nonlinearity of the flow is reduced. Indeed, Kraichnan and Panda[17] clearly demonstrated such a reduction by showing that the quantity $\langle|\nabla h_0+\mathbf{l}|^2\rangle$ is only about 57% of the corresponding value for a Gaussian field with the same energy spectrum (see review by Moffatt and Tsinober[18]).

In spite of these progresses, the transport of $\mathbf{l}$ and its mean fluctuation have never been fully explored, although the first such attempt was made as early as nearly seven decades ago by J. J. Thomson.[19] Based on an analogy between vortex filaments and electric-force lines, Thomson proposed to describe turbulence in terms of fluctuating vorticity $\boldsymbol{\omega}'$ and mean fluctuating Lamb vector $\overline{\mathbf{l}'}$, and suggested a model equation for $\overline{\mathbf{l}'}$. While Thomson's model was too simplified to be of any use, his idea was revived in a recent paper of Marmanis[20] who re-examined the analogy between the Navier–Stokes equations and Maxwell's equations and its application to turbulence. Our approach is somewhat different, with new formulation for RANS and LES in mind. In this section we examine the exact equations for $\mathbf{l}$ and $\overline{\mathbf{l}'}$.

A. Transport of full Lamb vector

Consider an incompressible flow of unit density, governed by

$$\frac{\partial \mathbf{u}}{\partial t}+\mathbf{l}=-\nabla h_0+\nu\nabla^2\mathbf{u}, \tag{7a}$$

$$\nabla\cdot\mathbf{u}=0, \tag{7b}$$

where $\mathbf{l}=\boldsymbol{\omega}\times\mathbf{u}$ is the Lamb vector and $h_0=p+|\mathbf{u}^2|/2$ the stagnation enthalpy. Based on (4), Eq. (7a) is split to

$$\frac{\partial \mathbf{u}}{\partial t}+\mathbf{l}_\perp=\nu\nabla^2\mathbf{u}, \tag{8a}$$

$$\mathbf{l}_\parallel=-\nabla h_0. \tag{8b}$$

Take the vector product of $\boldsymbol{\omega}$ and Eq. (7a), and that of the vorticity transport equation

$$\frac{\partial \boldsymbol{\omega}}{\partial t}+\nabla\times\mathbf{l}=\nu\nabla^2\boldsymbol{\omega}, \tag{9}$$

and $\mathbf{u}$, and make the sum of the results. After some algebra we find the exact transport equation for the full Lamb vector $\mathbf{l}$

$$\frac{\partial \mathbf{l}}{\partial t}+\mathbf{u}\cdot\nabla\mathbf{l}+\mathbf{l}\cdot\nabla\mathbf{u}-\nu\nabla^2\mathbf{l}=\nabla h_0\times\boldsymbol{\omega}+\nu\mathbf{q}, \tag{10}$$

where[4]

$$\mathbf{q}=-2\nu\boldsymbol{\omega}_{,k}\times\mathbf{u}_{,k}=\nu\nabla\cdot\boldsymbol{\tau}, \tag{11a}$$

$$\tau_{ij}=(u_{k,i}+u_{i,k})(u_{j,k}-u_{k,j})-\omega_i\omega_j, \tag{11b}$$

is a viscous source.[21]

An important mechanism of the $\mathbf{l}$ transport is the third term of Eq. (10) on the left, which represents the inviscid stretching and tilting with an opposite sign. The former deserves a further examination. It can be described by the variation of the scalar

$$J\equiv\tfrac{1}{2}|\mathbf{l}|^2=\tfrac{1}{2}(|\boldsymbol{\omega}|^2|\mathbf{u}|^2-\mathcal{H}^2), \tag{12}$$

where $\mathcal{H}\equiv\boldsymbol{\omega}\cdot\mathbf{u}$ is the helicity density. The transport equation for J reads

$$\frac{DJ}{Dt}+\mathbf{l}\cdot\mathbf{d}\cdot\mathbf{l}-\nu\nabla^2 J=-\nu\nabla\mathbf{l}:\nabla\mathbf{l}+Q_J, \tag{13}$$

where $\mathbf{d}$ is the strain-rate tensor, $\nu\nabla\mathbf{l}\colon\nabla\mathbf{l}$ is the J-dissipation, and

$$Q_J=(\mathcal{H}\boldsymbol{\omega}-|\boldsymbol{\omega}|^2\mathbf{u})\cdot\nabla h_0+\nu\mathbf{l}\cdot\mathbf{q}. \tag{14}$$

Because $\boldsymbol{\omega}\cdot\mathbf{l}=\mathbf{u}\cdot\mathbf{l}=0$, in Eq. (14) $\nabla h_0=-\mathbf{l}_\parallel$ can be replaced by $\mathbf{l}_\perp$. Denote $\mathbf{l}\cdot\mathbf{d}\cdot\mathbf{l}=\alpha J$ such that α is the opposite-sign stretching factor for $\mathbf{l}$. Because generically in a strain field a vector's stretching dominates shrinking, we expect $\alpha>0$ in average. This causes an inviscid reduction of J and hence implies that velocity and vorticity tend to be aligned. However, we shall see evidence that this tendency is counteracted by advection, and it is the competition of these two mechanisms that determines the inviscid evolution of $\mathbf{l}$. Consequently, a turbulence can hardly become fully Beltramian.[22]

We return to Eq. (10). By using Eq. (8b), there is

$$\nabla h_0\times\boldsymbol{\omega}=-\mathbf{l}_\parallel\times(\nabla\times\mathbf{u})=\mathbf{l}_\parallel\cdot\nabla\mathbf{u}+\nabla\mathbf{l}_\parallel\cdot\mathbf{u}+\nabla(\mathbf{u}\cdot\mathbf{l}_\perp),$$

where again we used the fact $\mathbf{u}\cdot\mathbf{l}_\parallel=-\mathbf{u}\cdot\mathbf{l}_\perp$. Thus

$$\begin{aligned}&\mathbf{u}\cdot\nabla\mathbf{l}+\mathbf{l}\cdot\nabla\mathbf{u}-\nabla h_0\times\boldsymbol{\omega}\\&\quad=\nabla\cdot(\mathbf{u}\mathbf{l}_\perp+\mathbf{l}_\perp\mathbf{u})-\nabla(\mathbf{u}\cdot\mathbf{l}_\perp)+\mathbf{u}\cdot\nabla\mathbf{l}_\parallel-\nabla\mathbf{l}_\parallel\cdot\mathbf{u},\end{aligned}$$

in which the last two terms are cancelled since $\nabla\mathbf{l}_\parallel=-\nabla\nabla h_0$ is a symmetric tensor. Therefore, Eq. (10) takes a more compact form:

$$\frac{\partial \mathbf{l}}{\partial t}+\nabla\cdot(\mathbf{u}\mathbf{l}_\perp+\mathbf{l}_\perp\mathbf{u})-\nu\nabla^2\mathbf{l}=\nabla(\mathbf{u}\cdot\mathbf{l}_\perp)+\nu\mathbf{q}. \tag{15}$$

The inviscid transport of $\mathbf{l}$ is now governed by advection and opposite-sign stretching–tilting of $\mathbf{l}_\perp$. Later in Sec. III A we shall recognize that $\nabla(\mathbf{u}\cdot\mathbf{l}_\perp)$ represents a ''residue'' of the advection of the gradient of kinetic energy (with a sign difference).

We project Eq. (15) into solenoidal space. Since

$$\nabla^2\mathbf{l}=\nabla(\nabla\cdot\mathbf{l})-\nabla\times\nabla\times\mathbf{l}=\nabla(\nabla\cdot\mathbf{l}_\parallel)+\nabla^2\mathbf{l}_\perp,$$

the transverse part of Eq. (15) reads

$$\frac{\partial \mathbf{l}_\perp}{\partial t}+[\nabla\cdot(\mathbf{u}\mathbf{l}_\perp+\mathbf{l}_\perp\mathbf{u})]_\perp-\nu\nabla^2\mathbf{l}_\perp=\nu\mathbf{q}_\perp. \tag{16}$$

Except viscous effect, $\mathbf{l}_\perp$ has no source or sink inside the flow field, similar to the case of vorticity or any other solenoidal field.

The longitudinal part of $\mathbf{l}$ follows from subtracting Eq. (16) from Eq. (15)

$$\frac{\partial \mathbf{l}_\parallel}{\partial t} - \nu\nabla(\nabla\cdot\mathbf{l}_\parallel) = \nabla(\mathbf{u}\cdot\mathbf{l}_\perp) - [\nabla\cdot(\mathbf{u}\mathbf{l}_\perp + \mathbf{l}_\perp\mathbf{u})]_\parallel + \nu\mathbf{q}_\parallel. \tag{17}$$

The second term on the left is similar to the longitudinal viscous effect in the compressible Navier–Stokes equation. Moreover, there must exist some $\Psi(\mathbf{l}_\perp)$ such that

$$\nabla(\mathbf{u}\cdot\mathbf{l}_\perp) - [\nabla\cdot(\mathbf{u}\mathbf{l}_\perp + \mathbf{l}_\perp\mathbf{u})]_\parallel + \nu\mathbf{q}_\parallel = -\nabla\Psi,$$

so from Eq. (17) we obtain an inhomogeneous linear diffusion equation for h_0

$$\left(\frac{\partial}{\partial t} - \nu\nabla^2\right)h_0 = \Psi(\mathbf{l}_\perp), \tag{18}$$

in which the integration constant (a function of time) is absorbed in Ψ.

B. Dominant mechanisms in Lamb vector evolution

Denoting

$$\mathcal{L} = \frac{\partial}{\partial t} - \nu\nabla^2,$$

and letting $\mathcal{L}^{-1}$ be its inverse (integral) operator, Eq. (8a) indicates that in Eq. (15) we may write

$$\nabla\cdot(\mathbf{u}\mathbf{l}_\perp + \mathbf{l}_\perp\mathbf{u}) = -\nabla\cdot[(\mathcal{L}^{-1}\mathbf{l}_\perp)\mathbf{l}_\perp + \mathbf{l}_\perp(\mathcal{L}^{-1}\mathbf{l}_\perp)].$$

The source $\nu\mathbf{q}$ can be similarly expressed through Eqs. (8a) and (9). Therefore, like the velocity $\mathbf{u}$ in Eq. (8a), $\mathbf{l}$ *is solely driven by* $\mathbf{l}_\perp$ *and its global history*. It is this nonlinear global and historical effect that causes most complicated evolution of all vortical flows including turbulence. This can also be seen from Eq. (17), where as sources the right-hand side is entirely from $\mathbf{l}_\perp$ and its global history. Thus, following the variation of $\mathbf{l}_\perp$, $\mathbf{l}_\parallel$ varies passively. $\mathbf{l}_\parallel$ is *neither advected nor stretched–tilted*. This is similar to the behavior of pressure gradient. However, unlike the pressure, because $\mathbf{l}_\parallel = -\nabla h_0$ contains kinetic energy, it is governed by an inhomogeneous linear diffusion equation.

In order to gain some taste of the key role of $\mathbf{l}_\perp$ in the evolution of Lamb vector, a preliminary numerical computation was made for the evolution of a perturbed periodic vortex array. A pseudo-spectral method was used in a cubic box of size 2π, with 64^3 coarse grid. The Reynolds number based on unperturbed vortex-core radius and maximum circumferential velocity was 10^5. The unperturbed basic flows was the ''frozen Oseen vortex,'' of which $\mathbf{l}_\perp = 0$ and $\mathbf{l}_\parallel$ is along the radial direction. To this basic flow we imposed an initial spiral perturbation at its axis containing six different nonaxisymmetric modes, with the maximal radial deviation from the z axis being 5% radius. We did not expect that small-scale eddies can be resolved by this coarse grid. Indeed, following the suggestion of a referee, we found that the spatial-averaged skewness and flatness factors of velocity field at the end of computation ($t=100$) are quite different from that in a fully resolved freely decaying turbulence. But the computation does give an evidence on what is happening in the evolution of Lamb vector.

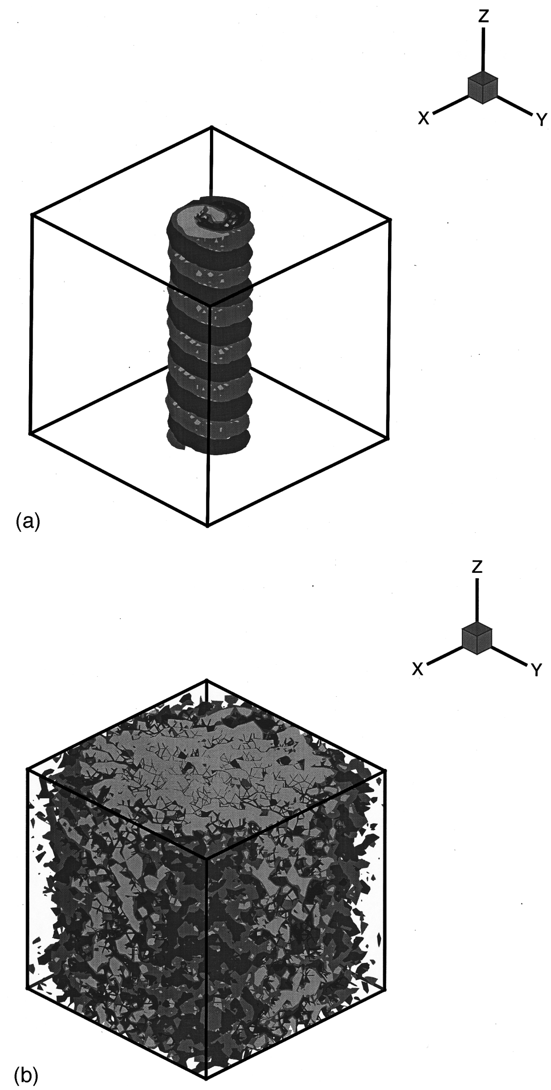

FIG. 1. Isosurfaces of helicity density $\boldsymbol{\omega}\cdot\mathbf{u} = (-0.1, 0.1)$ at (a) $t=1$ and (b) $t=40$.

The initial perturbation yields a small nonzero $\mathbf{l}_\perp$, which makes positive and negative helicity density $\mathcal{H} \equiv \boldsymbol{\omega}\cdot\mathbf{u}$ alternatively dominant in the vortex core. Figure 1 shows the isosurfaces of $\mathcal{H}$ at selected time of initial stage of evolution. The inside structure of $\mathcal{H}$ is more complicated, as seen from Fig. 2 for its (x,z) sectional contours. It is of interest that as time goes on the plot of $\mathcal{H}$ is gradually filled by its positive and negative extreme values, indicating a tendency of being Beltramian (but not completely). While our concern here is not exploring the specific physical process of vortex instability and transition to turbulence, it is worth mentioning that the unstable evolution shown in Figs. 1 and 2 is similar to those observed experimentally by Sarpakaya,[23] and numerically by, among others, Melander and Hussain,[24,25] Virk *et al.*,[26] and Sreedhar and Ragab.[27]

We concentrate on the time evolution of $\mathbf{l}$, $\mathbf{l}_\perp$, and $\mathbf{l}_\parallel$. Their space-averaged absolute values, denoted by $\langle|\cdot|\rangle$, are shown in Fig. 3 with a quite coarse time interval $\Delta t = 4$, which may have smeared out high-frequency fluctuations.

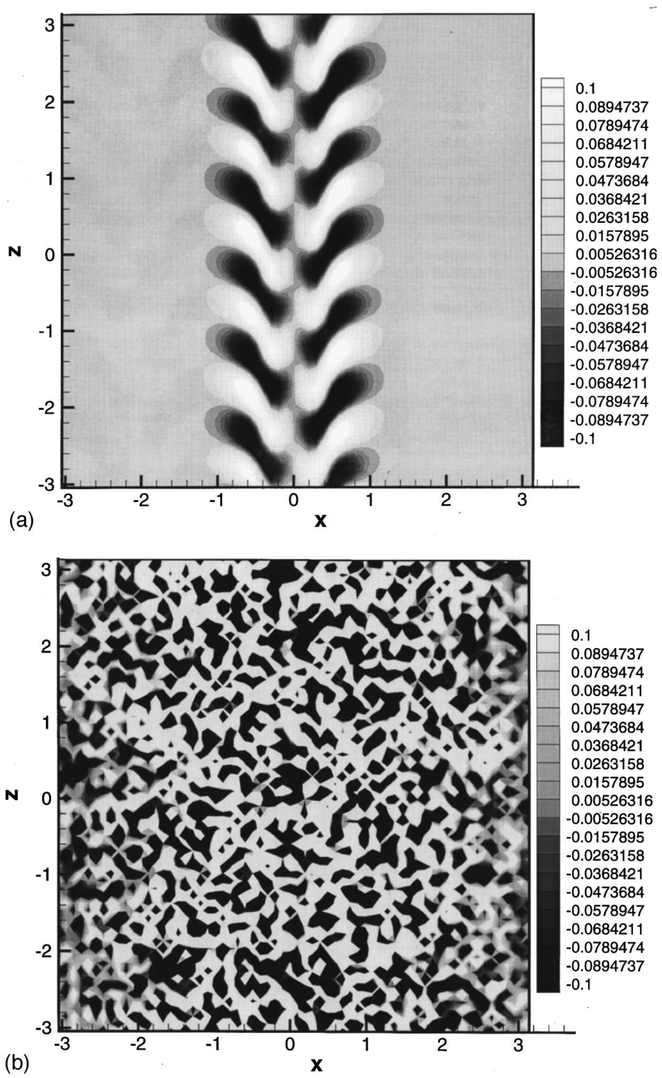

FIG. 2. Sectional contours of helicity density $\boldsymbol{\omega}\cdot\mathbf{u}$ on $y-z$ plane at (a) $t=1$ and (b) $t=40$. The unperturbed vortex axis is along the z direction. The minimum and maximum values of $\boldsymbol{\omega}\cdot\mathbf{u}$ are: (a) $(-0.160,\ 0.172)$; (b) $(-5.317,\ 7.247)$.

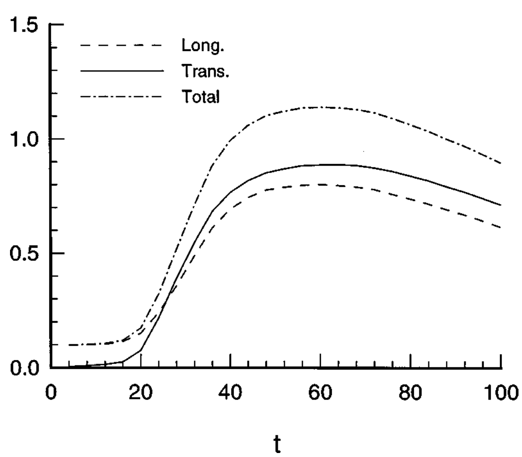

FIG. 3. Time evolution of spatially averaged absolute values of $\mathbf{l}_{\parallel}$, $\mathbf{l}_{\perp}$, and $\mathbf{l}$.

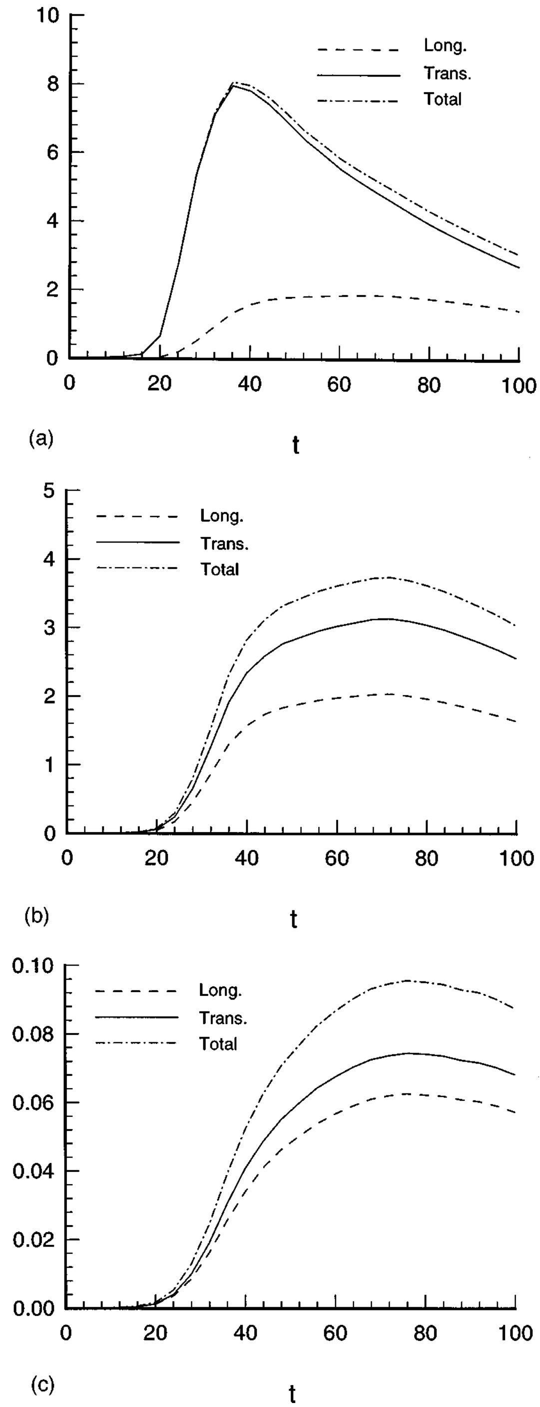

FIG. 4. Time evolution of spatially averaged absolute values of terms in equation (15): (a) $(\mathbf{u}\cdot\nabla\mathbf{l}_{\perp})_{\parallel}$, $(\mathbf{u}\cdot\nabla\mathbf{l}_{\perp})_{\perp}$, and $\mathbf{u}\cdot\nabla\mathbf{l}_{\perp}$; (b) $(\mathbf{l}_{\perp}\cdot\nabla\mathbf{u})_{\parallel}$, $(\mathbf{l}_{\perp}\cdot\nabla\mathbf{u})_{\perp}$, and $\mathbf{l}_{\perp}\cdot\nabla\mathbf{u}$; (c) $\nu\mathbf{q}_{\parallel}$, $\nu\mathbf{q}_{\perp}$, and $\nu\mathbf{q}$.

The figure indicates that although initially $|\mathbf{l}_{\perp}|\simeq 0$, it quickly grows and in average becomes larger than $|\mathbf{l}_{\parallel}|$. This confirms that, as predicted by the theory, the former drives the latter. After arriving their peak values, $\langle|\mathbf{l}|\rangle$, $\langle|\mathbf{l}_{\perp}|\rangle$, and $\langle|\mathbf{l}_{\parallel}|\rangle$ start to decrease. To see which effect of advection, stretching, and viscosity causes this decay most, Figs. 4(a)–4(c) show the corresponding evolution of the mean absolute values of $\mathbf{u}\cdot\nabla\mathbf{l}_{\perp}$, $\mathbf{l}_{\perp}\cdot\nabla\mathbf{u}$, and $\nu\mathbf{q}$, along with their transverse-longitudinal splitting. After a peak at $t\simeq 36$, there is a fast falling of $\langle|\mathbf{u}\cdot\nabla\mathbf{l}_{\perp}|\rangle$, which also drives the falling of $\langle|\mathbf{u}\cdot\nabla\mathbf{l}_{\parallel}|\rangle$. More significantly, unlike the advection, the entire trend of $\mathbf{l}_\perp$ and $\mathbf{l}$ (Fig. 3) is closely similar to that of Fig. 4(b). This demonstrates the key role of the opposite-sign stretching of $\mathbf{l}_\perp$. The viscous source/sink term $\nu\mathbf{q}$ is relatively small although larger than $O(Re^{-1})$. A similar level was found for the diffusion of $\mathbf{l}$ (not shown). However, the mild decay of $|\mathbf{l}|$ after $t=60$ may be due to the accumulated J-dissipation as indicated in Eq. (13).

Figures 5(a)–5(c) present the evolution of maximum local absolute values of $\mathbf{l}$ (taken from the computational domain) and its splitting, and that of transverse and longitudinal parts of $\mathbf{u}\cdot\nabla\mathbf{l}_\perp$ and $\mathbf{l}_\perp\cdot\nabla\mathbf{u}$. Here, two sharp peaks of $|(\mathbf{u}\cdot\nabla\mathbf{l}_\perp)_\perp|_{\max}$ and $|(\mathbf{l}_\perp\cdot\nabla\mathbf{u})_\perp|_{\max}$ are evident. Since the magnitude of these peaks are about 20 times of the mean values, the local events with vary large peaks must be relatively rare. Note that the peaks of $(\mathbf{l}_\perp\cdot\nabla\mathbf{u})_\perp$ have a time lag compared to that of $(\mathbf{u}\cdot\nabla\mathbf{l}_\perp)_\perp$. The most active mechanism of the fast growth of $(\mathbf{u}\cdot\nabla\mathbf{l}_\perp)_\perp$ is likely due to the vorticity enhancement by stretching at higher wave numbers—from Fig. 2 we saw that at $t=36$ the flow is already quite chaotic. This abrupt growth of $\mathbf{l}$ is then quickly upset by its induced stretching–tilting with opposite sign. The peak values of the latter is only about one-third of the former; but, because shrinking causes an exponential type of temporal decay of $|\mathbf{l}_\perp|$, a one-third level is sufficient to suppress the peak at a later time. The second peak at $t=40$ in Fig. 5(b) should be another similar process.

Figure 6 shows the three components of the vector $(\mathbf{u}\cdot\nabla\mathbf{l}_\perp)_\perp$ along the x axis, which is perpendicular to the vortex axis. The time is $t=32$, when the first peak appears. In the figure the components of $(\mathbf{u}\cdot\nabla\mathbf{l}_\perp)_\parallel$ are also plotted for comparison, which do not have strong fluctuations. The locations of $(\mathbf{u}\cdot\nabla\mathbf{l}_\perp)_\parallel$ peaks are near the outer edge of the core, known to be about the most unstable region of a disturbed vortex where circumferencial vortex filaments spiral out.[23] The same components along the vortex axis (not shown) have much smaller peaks. A corresponding fluctuation of $(\mathbf{l}_\perp\cdot\nabla\mathbf{u})_\perp$ at $t=36$ (when its strong peaks occur), compared with that of $(\mathbf{l}_\perp\cdot\nabla\mathbf{u})_\parallel$, is shown in Fig. 7. In contrast to Figs. 5–7, for $\mathbf{l}_\perp$ and $\mathbf{l}_\parallel$ at these times we saw no strong fluctuations (not shown).

C. Transport of mean fluctuating Lamb vector

Returning to turbulent force, we split the velocity, vorticity, and pressure into a mean part and a fluctuating part

$$\mathbf{u}=\mathbf{U}+\mathbf{u}', \quad \boldsymbol{\omega}=\boldsymbol{\Omega}+\boldsymbol{\omega}', \quad p=P+p', \tag{19}$$

such that

$$\overline{(\boldsymbol{\Omega}+\boldsymbol{\omega}')\times(\mathbf{U}+\mathbf{u}')}=\mathbf{L}+\overline{\mathbf{l}'}, \tag{20a}$$

$$\overline{(P+p')+(|\mathbf{U}+\mathbf{u}'|^2)/2}=H_0+K, \tag{20b}$$

where

$$\mathbf{L}=\boldsymbol{\Omega}\times\mathbf{U}, \tag{21a}$$

$$H_0=P+\tfrac{1}{2}|\mathbf{U}|^2, \tag{21b}$$

are the mean Lamb vector and stagnation enthalpy, and $\overline{\mathbf{l}'}$ and K are defined by Eqs. 3(a) and 3(b). Substituting Eq. (20) into Eqs. (8a) and (8b), for the mean flow there is

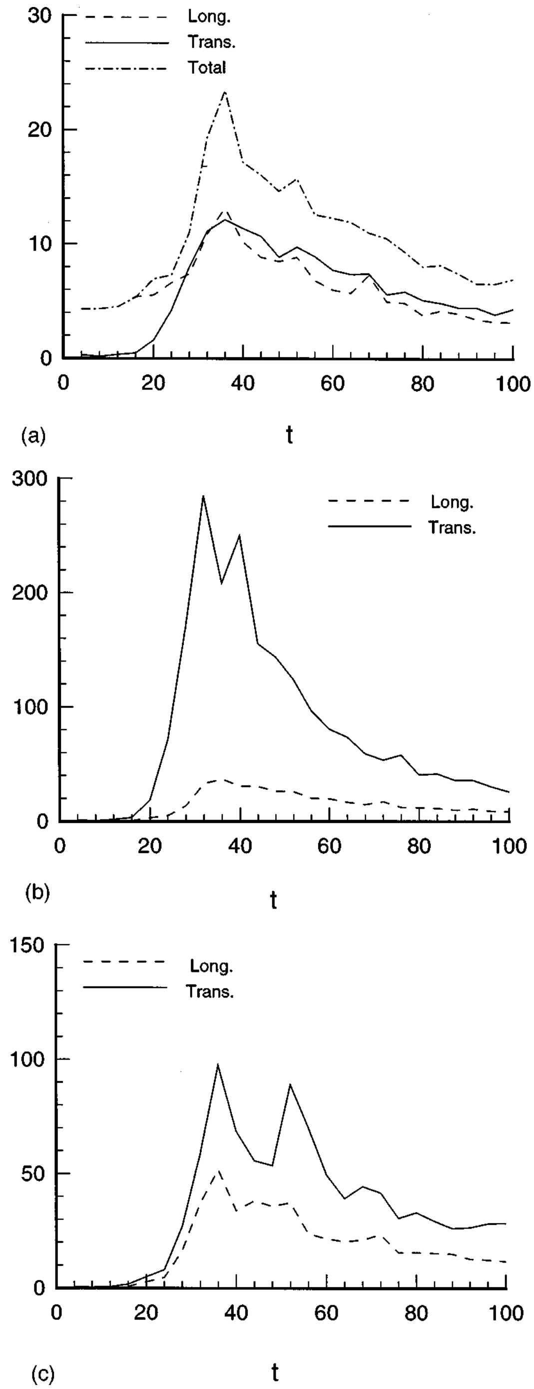

FIG. 5. Time evolution of maximum absolute values of: (a) $\mathbf{l}_\parallel$, $\mathbf{l}_\perp$, and $\mathbf{l}$; (b) $(\mathbf{u}\cdot\nabla\mathbf{l}_\perp)_\parallel$ and $(\mathbf{u}\cdot\nabla\mathbf{l}_\perp)_\perp$; (c) $(\mathbf{l}_\perp\cdot\nabla\mathbf{u})_\parallel$ and $(\mathbf{l}_\perp\cdot\nabla\mathbf{u})_\perp$.

$$\frac{\partial\mathbf{U}}{\partial t}+\mathbf{L}_\perp=-\overline{\mathbf{l}'}_\perp+\nu\nabla^2\mathbf{U}, \tag{22a}$$

$$\mathbf{L}_\parallel=-\nabla H_0-(\overline{\mathbf{l}'_\parallel}+\nabla K). \tag{22b}$$

Note that comparing Eqs. (22a) and (22b) and Eq. (1a) recovers Eqs. (2), (6a), and (6b).

Now, by comparing Eqs. (22a) and (8a), and following the same procedure of deriving Eq. (15), we obtain the transport equation for $\mathbf{L}$:

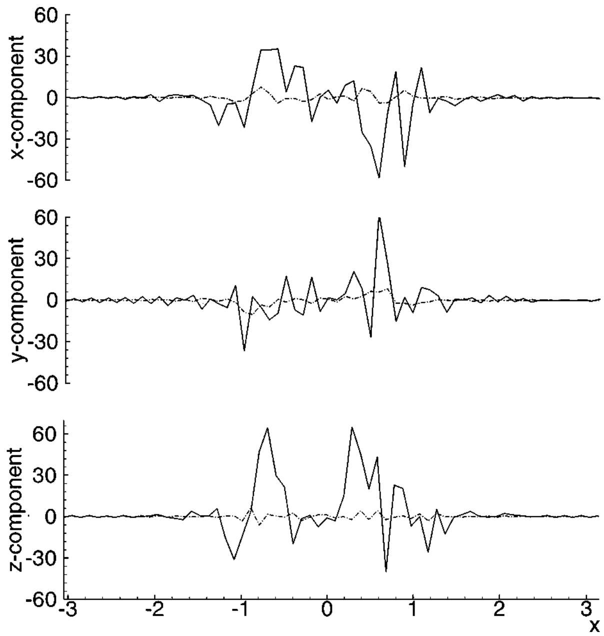

FIG. 6. The (x,y,z) components of $(\mathbf{u}\cdot\nabla\mathbf{l}_\perp)_\perp$ and $(\mathbf{u}\cdot\nabla\mathbf{l}_\perp)_\parallel$ on the x axis perpendicular to the vortex axis at $t=32$.

$$\frac{\partial\mathbf{L}}{\partial t}+\nabla\cdot[\mathbf{U}(\mathbf{L}_\perp+\overline{\mathbf{l}'}_\perp)+(\mathbf{L}_\perp+\overline{\mathbf{l}'}_\perp)\mathbf{U}]$$
$$=\nabla[\mathbf{U}\cdot(\mathbf{L}_\perp+\overline{\mathbf{l}'}_\perp)]+\nu\nabla^2\mathbf{L}+\nu\mathbf{Q}, \tag{23}$$

where $\mathbf{Q}$ has the same form as Eq. (11) but with $\mathbf{u}$ and $\boldsymbol{\omega}$ replaced by $\mathbf{U}$ and $\boldsymbol{\Omega}$, respectively. The term $\nabla\cdot(\mathbf{U}\overline{\mathbf{l}'}_\perp+\overline{\mathbf{l}'}_\perp\mathbf{U})$ is analogous to the Reynolds stress in RANS equation. Equation (23) will be closed once $\overline{\mathbf{l}'}_\perp$ is known.

To obtain the equation for $\overline{\mathbf{l}'}$, then, we take ensemble average of Eq. (15) and then subtract Eq. (23). Define a ''*pseudo-Lamb vector*''

$$\mathbf{L}'\equiv(\boldsymbol{\Omega}+\boldsymbol{\omega}')\times\mathbf{u}'+\boldsymbol{\omega}'\times\mathbf{U}, \tag{24}$$

which represents the rotation of $\mathbf{u}'$ by $\boldsymbol{\Omega}+\boldsymbol{\omega}'$ and $\mathbf{U}$ by $\boldsymbol{\omega}'$. It contains both mean and fluctuating quantities, and hence the notation. Then for any quantity $v=V+v'$, there is

$$\overline{v\mathbf{l}}=\overline{(V+v')[(\boldsymbol{\Omega}+\boldsymbol{\omega}')\times(\mathbf{U}+\mathbf{u}')]}=V(\mathbf{L}+\overline{\mathbf{l}'})+\overline{v'\mathbf{L}'}. \tag{25}$$

Thus, a very neat equation for $\overline{\mathbf{l}'}$ follows:

$$\left(\frac{\partial}{\partial t}-\nu\nabla^2\right)\overline{\mathbf{l}'}=\nabla\cdot\mathbf{S}_l. \tag{26}$$

Here, the source tensor $\mathbf{S}_l$ is given by

$$\mathbf{S}_l=\mathbf{I}(\overline{\mathbf{u}'\cdot\mathbf{L}'_\perp})-(\overline{\mathbf{u}'\mathbf{L}'_\perp+\mathbf{L}'_\perp\mathbf{u}'})+\nu\overline{\boldsymbol{\tau}'}, \tag{27}$$

in which $\mathbf{I}$ is the unit tensor and $\boldsymbol{\tau}'$ has the same form as in Eq. (11b) but uses fluctuating quantities.[28] The vector $\nabla\cdot\mathbf{S}_l$ contains both double and triple correlations and has to be modeled. The most remarkable feature is that $\overline{\mathbf{l}'}$ is not advected by $\mathbf{U}$ *in this equation*. It *is* so, though, which however, has to appear (and only appears) in the mean-Lamb vector Eq. (23) just like the turbulent force has to appear in Eqs. (22a) and (22b) or Eq. (1a).

III. MEAN FLUCTUATING KINETIC ENERGY AND TURBULENT FORCE

In the preceding section we examined the transport of the major part of turbulent force, i.e., the first term of Eq. (2). To complete the theory we now turn to the second term.

A. Mean fluctuating kinetic energy

In contrast to Eq. (26) which holds only for $\overline{\mathbf{l}'}$ but not $\mathbf{l}$, in a recent note Wu *et al.*[29] prove that even the full kinetic-energy E can be cast to a diffusion equation

$$\left(\frac{\partial}{\partial t}-\nu\nabla^2\right)E=-\mathbf{l}_\perp\cdot\mathbf{u}-\frac{1}{2}(\Phi+\nu|\boldsymbol{\omega}|^2), \tag{28}$$

where $\Phi=2\nu\mathbf{d}\colon\mathbf{d}$ is the dissipation. Owing to starting from projected Eq. (8a) instead of Eq. (7a), the nonlinear velocity advection $\mathbf{u}\cdot\nabla\mathbf{u}$ only leaves a ''residue'' $\mathbf{l}_\perp$. Consequently, the advection of kinetic energy, $\mathbf{u}\cdot\nabla E$, leaves a residue $\mathbf{l}_\perp\cdot\mathbf{u}$ in Eq. (28). The pressure work is entirely removed by projection, and the viscous work-rate done by shear stress is partially cast to the diffusion of E and partially causes the simultaneous appearance of dissipation and enstrophy. Some interesting implications of Eq. (28) relevant to turbulence theory has been briefly discussed in Ref. 29; here we focus on its mean fluctuating part. As before, we split the quantities in Eq. (28) into mean and fluctuating parts such that $\mathbf{d}=\mathbf{D}+\mathbf{d}'$, etc. Then the mean kinetic-energy equation reads

$$\left(\frac{\partial}{\partial t}-\nu\nabla^2\right)\frac{1}{2}|\mathbf{U}|^2=-(\mathbf{L}_\perp+\overline{\mathbf{l}'}_\perp)\cdot\mathbf{U}-\frac{\nu}{2}(2\mathbf{D}\colon\mathbf{D}+|\boldsymbol{\Omega}|^2), \tag{29}$$

where $-\overline{\mathbf{l}'}_\perp\cdot\mathbf{U}$ is the energy exchange between the mean flow and fluctuations. The direction of this energy flux is simply determined by the relative orientation of $\mathbf{U}$ and $\overline{\mathbf{l}'}_\perp$. Then, since

$$2\nu\mathbf{d}\colon\mathbf{d}=\nu|\boldsymbol{\omega}|^2+2\nu\nabla\cdot(\mathbf{u}\cdot\nabla\mathbf{u})=\nu|\boldsymbol{\omega}|^2-2\nu\nabla^2p,$$

but $\overline{p'}=0$, there is $2\nu\overline{\mathbf{d}'\colon\mathbf{d}'}=\nu\overline{|\boldsymbol{\omega}'|^2}$. Hence, by using Eqs. (24) and (25) we obtain a general mean fluctuating energy equation

$$\left(\frac{\partial}{\partial t}-\nu\nabla^2\right)K=-\overline{\mathbf{L}'_\perp\cdot\mathbf{u}'}-\nu\overline{|\boldsymbol{\omega}'|^2}. \tag{30}$$

B. Turbulent force as a forced diffusive field

The desired equation for turbulent force $\mathbf{f}$ is simply the sum of Eq. (26) and the gradient of Eq. (30). The latter reads

$$\left(\frac{\partial}{\partial t}-\nu\nabla^2\right)\nabla K=\nabla\cdot\mathbf{S}_K, \tag{31}$$

where

$$\mathbf{S}_K=-\mathbf{I}(\overline{\mathbf{L}'_\perp\cdot\mathbf{u}'}+\nu\overline{|\boldsymbol{\omega}'|^2}). \tag{32}$$

Therefore, the final form of turbulent-force equation reads

$$\left(\frac{\partial}{\partial t}-\nu\nabla^2\right)\mathbf{f}=\nabla\cdot\mathbf{S}, \tag{33}$$

where

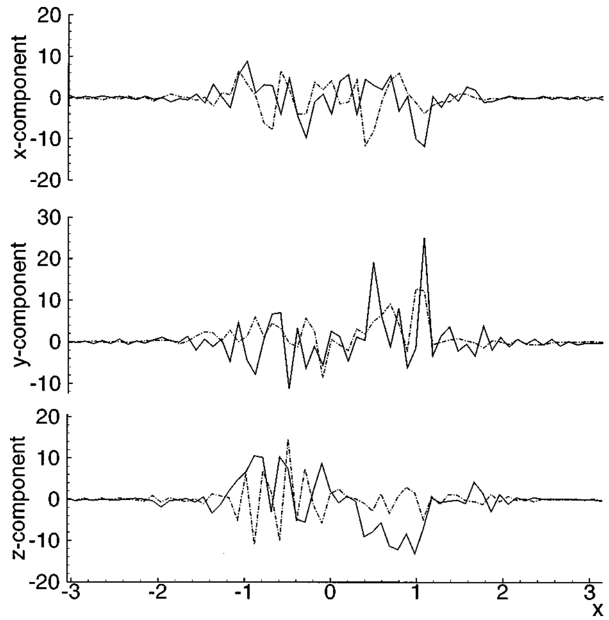

FIG. 7. The (x,y,z) components of $(\mathbf{l}_\perp\cdot\nabla\mathbf{u})_\perp$ and $(\mathbf{l}_\perp\cdot\nabla\mathbf{u})_\parallel$ on the x axis at $t=36$.

$$\mathbf{S}=\mathbf{S}_l+\mathbf{S}_K=-(\overline{\mathbf{u}'\mathbf{L}'_\perp+\mathbf{L}'_\perp\mathbf{u}'})+\nu(\overline{\boldsymbol{\tau}'}-\mathbf{I}\overline{|\boldsymbol{\omega}'|^2}), \tag{34}$$

which completes our theoretical development. Equations (33) and (34) can also be derived from taking the sum of Eq. (15) and gradient of Eq. (28) first and then subtracting the mean part.

This new equation of turbulent force is closely similar to Lighthill's acoustic analogy,[30] in the sense that both are exact and in both one deals with classic linear equations with constant coefficients, leaving all nonlinear terms to the sources. While Lighthill's theory was a result of choosing proper variable (fluctuating density) for aerodynamic sound, now Eqs. (33) and (34) come from identifying the key role of Lamb vector. A difference is, however, for sound waves several choices of variables are equally permissible (such as pressure or stagnation enthalpy) but lead to different equations with variable complexity,[31] here $\overline{\mathbf{l}'}$ appears inevitably once we consider the vortical form of the Navier–Stokes equation.

The above formulation has a few significant characters:

(i) Although the mean fluctuating Lamb vector $\overline{\mathbf{l}'}$ is both advected and stretched (with opposite sign) by the mean flow $\mathbf{U}$, these mechanisms appear only in the transport Eq. (23) of $\mathbf{L}$ but not in its own transport Eq. (26). Similar situation happens for the advection of mean fluctuating kinetic energy K by $\mathbf{U}$, where the ''residue'' of this advection appears only in Eq. (29) but not Eq. (31). Consequently, both $\overline{\mathbf{l}'}$ and ∇K, and hence the turbulent force, behave more like a field rather than a material quantity. It is diffused only by *molecular viscosity*. This is a big deviation from conventional thinking and formulations (e.g., Ref. 3). It would be very interesting to examine whether the absence of advection of $\mathbf{f}$ by $\mathbf{U}$, along with a careful modeling of the source $\nabla\cdot\mathbf{S}$ to avoid simply attributing it to an eddy viscosity, could alleviate the problem mentioned in Sec. I that several popular RANS models smear too much some key large-scale vortical structures.

(ii) The longitudinal part of turbulent force, including kinetic energy, is passively driven by the transverse part and completely decoupled from the latter's evolution [see the remark following Eqs. (4a) and (4b)], unless the modeled $\nabla\cdot\mathbf{S}$ contains this coupling. This observation reinforces our assertion that the focus of turbulence modeling should be shifted from scalar equations to vortical vector equations.

(iii) All source (sink) terms in Eq. (34) are vortical, which vanish if $\boldsymbol{\omega}'=0$. This fact explicitly reconfirms the very truth: *No random vortices, no turbulence*. There is no correlation with pressure. It should be stressed that, although in Eqs. (27) or (34) correlations such as $\overline{\mathbf{u}'\mathbf{u}'}$ and $\overline{\mathbf{u}'\boldsymbol{\omega}'}$ are as complicated as or even more so than the Reynolds stress, writing the source terms as a divergence of a tensor is merely for neatness. Once again it suffices to think of three-component vector $\nabla\cdot\mathbf{S}$ only. The physics involved in the inviscid part of this source term is then immediately clear: the mean effect of advection and opposite-sign stretching of $\mathbf{L}'_\perp$ by the $\mathbf{u}'$-field.

IV. CONCLUDING REMARKS

In Reynolds averaged Navier–Stokes equation it suffices to compute the turbulent force rather than Reynolds stress tensor. The former is dominated by the mean fluctuating Lamb vector plus a contribution of mean fluctuating kinetic energy. This basic observation strongly suggests that it would be of great value to develop Lamb-vector based turbulence models at various orders of closure.

The transport equations of Lamb vector $\mathbf{l}$ and its projected parts are derived. It is shown that $\mathbf{l}_\perp$ and its global history is the unique driving mechanism of the flow. This transverse Lamb vector is in turn driven by the competition between its nonlinear advection and opposite-sign stretching–tilting, decoupled from any longitudinal part of the flow field.

Of particular interest is the linear inhomogeneous diffusion equation for the mean fluctuating Lamb vector $\overline{\mathbf{l}'}$, which presents a similarity with Lighthill's acoustic analogy. The transport equation for mean fluctuating kinetic energy can also be cast to the same form. Therefore, the turbulent force appears as an inhomogeneous diffusive vector field, diffused only by molecular viscosity and driven by vortical sources (mainly the advection and opposite-sign stretching of transverse pseudo-Lamb vector $\mathbf{L}'_\perp$ by the fluctuating velocity field). This diffusion equation is a natural logical consequence of the RANS equation, as long as we do the following:

(i) Focus on turbulent force $\mathbf{f}$ rather than the oversimplified energy-dissipation consideration, or the possibly overcomplicated consideration based on full Reynolds stress tensor;

(ii) Identify the two physical constituents of $\mathbf{f}$ as $\overline{\mathbf{l}'}$ and ∇K; and

(iii) Utilize the SH decomposition to work in solenoidal space as much as possible.

It is hoped that based on this new formulation turbulence models could be developed at an adequate complexity level between two-equation models and second-order closure. With minor modification, this formulation can also be applied to large-eddy simulation.

ACKNOWLEDGMENTS

The work is supported in part by Office of Naval Research under the Grant W00014-96-1-0452, and the National Aeronautics and Space Administration under NASA Contract No. NAS1-19480 while the first (J.Z.W. as a summer visitor) and second authors were in residence at the Institute for Computer Applications in Science and Engineering, NASA Langley Research Center. The major numerical computation was performed at NAS Eagle Cray C-90 supercomputer, NASA Ames Research Center. The third and fourth authors are grateful to the financial support of J. M. Wu Research Fund of UTSI and Peking University, Peking, China, respectively, during their stay at UTSI. Valuable discussions with Xiao-Hui Wu, Xie-Yuan Yin, Philippe Spalart, and H. Marmanis are very appreciated.

[1] P. R. Spalart, W.-H. Jou, M. Strelets, and S. R. Allmaras, ''Comments on the feasibility of LES for wings, and on a hybrid RANS/LES approach,'' 1st AFOSR Intern. Conf. on DNS/LES, 4–8 Aug. 1997, Ruston, Louisiana, in *Advances in DNS/LES*, edited by C. Liu and Z. Liu (Greyden, Columbus, OH, 1997).

[2] J. Z. Wu, X. Y. Lu, A. G. Denny, M. Fan, and J. M. Wu, ''Post-stall flow control on an airfoil by local unsteady forcing,'' J. Fluid Mech. **371**, 21 (1998).

[3] C. G. Speziale, ''Analytical methods for the development of Reynolds stress closures in turbulence,'' Annu. Rev. Fluid Mech. **23**, 107 (1991).

[4] J. Z. Wu, Y. Zhou, and J. M. Wu, ''Reduced stress tensor and dissipation and the transport of Lamb vector,'' ICASE Report 96-21 (1996).

[5] B. Perot and P. Moin, ''A new approach to turbulence,'' Proc. Summer Program, Center for Turbulence Research (1996).

[6] S. K. Lele, ''Vorticity form of turbulence transport equations,'' Phys. Fluids A **4**, 1767 (1992).

[7] H. Lamb, *Hydrodynamics* (Dover, New York, 1932).

[8] G. K. Batchelor, *An Introduction to Fluid Dynamics* (Cambridge University Press, Cambridge, 1967).

[9] H. K. Moffatt, *Topological Fluid Mechanics*, edited by A. Tsinober (Cambridge University Press, Cambridge, 1990).

[10] R. L. Ricca and M. A. Berger, ''Topological ideas and fluid mechanics,'' Phys. Today (Dec. 1996).

[11] H. K. Moffatt, ''On the existence of localized rotational disturbances which propagate without change of structure in an inviscid fluid,'' J. Fluid Mech. **173**, 289 (1986).

[12] H. K. Moffatt, ''Magnetostatic equilibria and analogous Euler flows of arbitrarily complex topology. Part 1. Fundamentals,'' J. Fluid Mech. **159**, 359 (1985).

[13] H. K. Moffatt, ''Magnetostatic equilibria and analogous Euler flows of arbitrarily complex topology. Part 2. Stability considerations,'' J. Fluid Mech. **166**, 359 (1986).

[14] V. Anol'd, ''The asymptotic Hopf invariant and its applications'' (in Russian), in Proc. Summer School in Differential Equations, Erevan, Armenian SSR Acad. Sci. (1974).

[15] A. Tsinober, ''On one property of Lamb vector in isotropic turbulent flow,'' Phys. Fluids A **2**, 484 (1990).

[16] L. Shtilman, ''On the solenoidality of the Lamb vector,'' Phys. Fluids A **4**, 197 (1992).

[17] R. H. Kraichnan and R. Panda, ''Depression of nonlinearity in decaying isotropic turbulence,'' Phys. Fluids **31**, 2395 (1988).

[18] H. K. Moffat and A. Tsinober, ''Helicity in laminar and turbulent flow,'' Annu. Rev. Fluid Mech. **24**, 281 (1992).

[19] J. J. Thomson, ''On the analogy between the electromagnetic field and a fluid containing a large number of vortex filaments,'' Philos. Mag. **12**, 1057 (1931).

[20] H. Marmanis, ''Analogy between the Navier–Stokes equations and Maxwell's equations: application to turbulence,'' Phys. Fluids **10**, 1428 (1998).

[21] It is easily shown that the second term of the viscous source $\nu\mathbf{q}$ is essentially due to a nonuniform distribution of enstrophy along vortex tubes and the tilting of the tubes.

[22] One might think that the competition between advection and stretching of $\mathbf{l}$ would be better understood in terms of more elementary processes such as the variation of vorticity $\boldsymbol{\omega}$, helicity density $\mathcal{H}$, and kinetic energy $E \equiv |\mathbf{u}|^2/2$. Then $\mathbf{u}\cdot\nabla J+\mathbf{l}\cdot\mathbf{d}\cdot\mathbf{l}$ in Eq. (14) can be cast to four terms. Unfortunately, the effect of two terms is hard to identify. Thus, we continue to study the Lamb vector as a whole.

[23] T. Sarpkaya, ''Vorticity, free surface, and surfactants,'' Annu. Rev. Fluid Mech. **28**, 83 (1996).

[24] M. V. Melander and F. Hussain, ''Cross-linking of two antiparallel vortex tubes,'' Phys. Fluids A **1**, 633 (1989).

[25] M. V. Melander and F. Hussain, ''Polarized vorticity dynamics on a vortex column,'' Phys. Fluids A **5**, 1992 (1993).

[26] D. Virk, F. Hussain, and R. M. Kerr, ''Compressible vortex reconnection,'' J. Fluid Mech. **304**, 47 (1995).

[27] M. K. Sreedhar and S. A. Ragab, ''Large eddy simulation of a longitudinal vortex,'' AIAA Paper 94-0529 (1994).

[28] Ref. 4 has derived Eq. (15) but failed to get the neat equation [Eq. (26)] due to an algebraic error.

[29] J. Z. Wu, Y. Zhou, and M. Fan, ''A note on kinetic energy, dissipation, and enstrophy,'' Phys. Fluids **11**, No 2, to appear.

[30] M. J. Lighthill, ''On sound generation aerodynamically. I. General theory,'' Proc. R. Soc. London, Ser. A **221**, 564 (1952).

[31] D. G. Crighton, ''Acoustics as a branch of fluid mechanics,'' J. Fluid Mech. **106**, 261 (1981).